

Preparation and Crystal Structure Analysis of $\text{Ba}_2\text{BiGa}_{11}\text{O}_{20}$

T. R. Wagner¹ and T. J. Styraneć

Department of Chemistry, Youngstown State University, Youngstown, Ohio 44555

Received September 22, 1997; in revised form February 2, 1998; accepted February 17, 1998

X-ray structure investigations of ternary $\text{BaO-Ga}_2\text{O}_3$ crystals grown in a Bi_2O_3 flux led to discovery of a quaternary compound of ideal composition $\text{Ba}_2\text{BiGa}_{11}\text{O}_{20}$. Single-crystal X-ray diffraction indicates a monoclinic unit cell with parameters $a = 14.9283(14)$ Å, $b = 11.7046(8)$ Å, $c = 5.1170(5)$ Å, and $\beta = 91.137(7)^\circ$. The structure is similar to that of $\text{Ba}_3\text{TiAl}_{10}\text{O}_{20}$ and related compounds. Three different refinement trials were completed, involving different treatments of positioning of bismuth or gallium atoms shifted from normal barium and gallium sites. The refinement selected as representing the best model has only one bismuth atom positioned near a barium site at a displacement of 0.495 Å. A crystal chemical analysis based on the X-ray data suggests that the displacement of bismuth atoms is due to the stereochemical activity of the $6s^2$ lone pair. X-ray refinement was carried out by full-matrix least squares on F^2 on all data, to give $R_1 = 0.0689$ and $wR_2 = 0.1802$ for 104 parameters and 1361 independent reflections. The final position assignments were analyzed via bond valence sum calculations. Other crystal data: $M = 1570.58$, space group $I2/m$ (No. 12), $V = 893.92(14)$ Å³, $Z = 2$, $D_c = 5.835$ g cm⁻³, $\text{MoK}\alpha = 0.71073$ Å, $\mu = 30.506$ mm⁻¹, $2\theta_{\text{max}} = 59.98^\circ$. © 1998 Academic Press

INTRODUCTION

During the course of X-ray structure investigations of single crystals in the ternary $\text{BaO-Ga}_2\text{O}_3$ system prepared from a Bi_2O_3 flux, monoclinic crystals representing a new phase for the system were discovered. The ideal composition of this phase was assigned as $\text{Ba}_2\text{BiGa}_{11}\text{O}_{20}$, by analogy to the growth of a monoclinic $\text{Sr}_2\text{BiGa}_{11}\text{O}_{20}$ phase reported by Haberey *et al.* (1) during preparation of $\text{SrGa}_{12}\text{O}_{19}$ crystals from a Bi_2O_3 flux. Although neither the unit cell parameters nor structure for this phase was reported, its formula is closely related to the general formula $A_3BC_{10}\text{O}_{20}$, for which several phases (with $A = \text{Sr, Ba, and Pb}$; $B = \text{Si, Ge, Sn, and Ti}$; and $C = \text{Al, Ga, and Fe}$) have been previously

studied (2–4) due largely to interest in their luminescence properties. All of these phases crystallize in the monoclinic system with cell parameters very similar to those obtained here for $\text{Ba}_2\text{BiGa}_{11}\text{O}_{20}$, suggesting that the compounds are isostructural. In the $A_3BC_{10}\text{O}_{20}$ compounds, the tetravalent B -type atoms share positions with the trivalent C -type atoms. Of interest in this study was the positioning of the Bi atoms, since Bi is trivalent and intermediate in size between Ba and Ga and has a $6s^2$ lone pair which can be stereochemically active. This is apparently the first detailed crystallographic characterization of this composition type, which could be generally represented as $A_2BC_{11}\text{O}_{20}$.

The major structural feature of the $A_3BC_{10}\text{O}_{20}$ compounds is a tetrahedral framework consisting of layers of ribbed planes of tetrahedra two tetrahedral units wide, with the layers “stacked” along the a axis as shown in Fig. 1. The successive layers are related by the twofold symmetry along the b axis. In Fig. 2, it is seen that each tetrahedral layer consists of a string (parallel to the c axis) of six-membered rings of corner-shared tetrahedra all with apices pointing in one direction (i.e., roughly parallel to the a axis), connected to two adjacent strings of six-membered rings at apices pointing in the opposite direction. That is, the six-membered rings in each of the two planes of the tetrahedral layer are not aligned, so that six apical oxygens of one ring bind to three oxygens from each of two strings in the adjacent plane. This results in a triangular inner space between the tetrahedral planes rather than the hexagonal inner space enclosed by the six-membered rings seen in β -tridymite, for example (4).

There are two types of large cation sites associated with these ribbed planes: the $A(1)$ -type site is located between the layers of ribbed planes in octahedral coordination, and the $A(2)$ -type site is positioned between the tetrahedral sheets (i.e., on roughly the same plane as the apical oxygens) with a coordination of 7, 8, or 9, depending on the composition (2–4). Besides the $A(1)$ cation, successive layers of ribbed tetrahedral planes are linked together by corner-sharing to a chain of octahedra which runs parallel to the c axis. Note that the atomic position numbering convention used here and throughout is the same as used by Cadée *et al.* (3) for $\text{Ba}_3\text{TiAl}_{10}\text{O}_{20}$.

¹ To whom correspondence should be addressed.

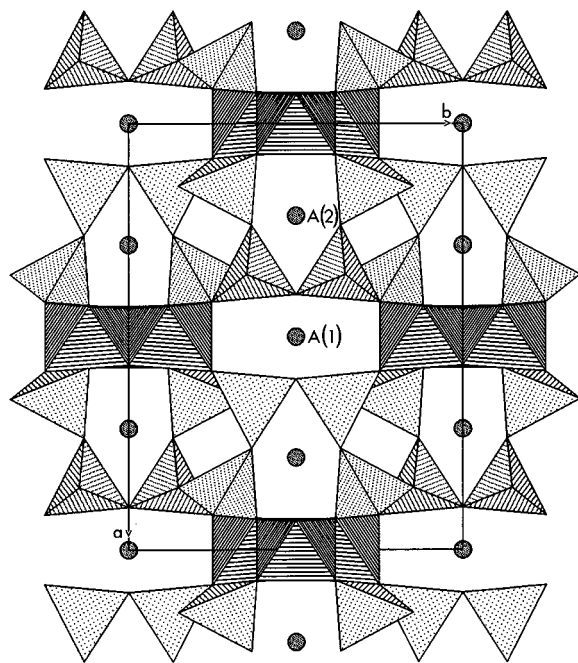


FIG. 1. Projection of the $A_3BC_{10}O_{20}$ -type structure along [001]. Successive layers of ribbed planes of tetrahedra, which are two tetrahedral units wide, are joined along the a direction by chains of octahedra and $A(1)$ -type atoms.

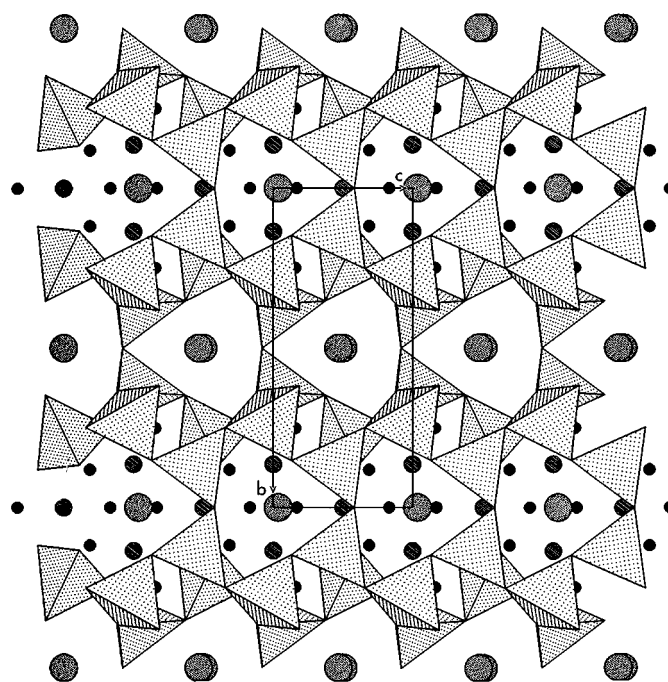


FIG. 2. Projection of the $A_3BC_{10}O_{20}$ structure along [100] showing strings of six-membered tetrahedral rings running along the c direction and joined at apical oxygens to two adjacent strings in the layer below. Large spheres are A atoms, small spheres are O atoms, and intermediate-sized spheres are C (or B)-type atoms in octahedral coordination.

EXPERIMENTAL

Sample Preparation

Single crystals were prepared from a Bi_2O_3 flux, utilizing the procedure outlined by Haberey *et al.* (1) for the preparation of single crystals of $SrGa_{12}O_{19}$. A 20/50/30 mol% mixture of $BaCO_3/Ga_2O_3/Bi_2O_3$ was heated in air in a covered Pt crucible at a rate of $60^\circ C/h$ to a temperature of $1350^\circ C$, where it was held for 5 h. The mixture was then cooled to $500^\circ C$ at a rate of $20^\circ C/h$ and finally to room temperature at a rate of $50^\circ C/h$. Preliminary X-ray characterizations indicated that the products consisted of colorless crystals of Ga_2O_3 , yellowish-green crystals of $BaGa_{12}O_{19}$, and yellowish-brown crystals of $Ba_2BiGa_{11}O_{20}$. The $Ba_2BiGa_{11}O_{20}$ crystal selected for analysis was an irregular polygonal platelet of approximate dimensions $0.33\text{ mm} \times 0.26\text{ mm} \times 0.03\text{ mm}$.

Structure Determination

X-ray data were collected on a Siemens P4 diffractometer equipped with a normal-focus, 3.0-kW sealed-tube X-ray source (Mo $K\alpha$ radiation, $\lambda = 0.71073\text{ \AA}$) operating at 55 kV and 45 mA. Unit cell dimensions were determined by a least-squares fit of 93 centered reflections with $12.998^\circ < 2\theta < 28.091^\circ$. A full sphere of intensity data was collected using a $\theta/2\theta$ scan. Siemens' analytical face-indexing routine

(in XSCANS version 2.10b) was used to index crystal faces for quantitative absorption corrections. The choice of space group was straightforward, with systematic absences indicating $C2/m$ (No. 12) symmetry. The $I2/m$ setting was chosen for the remainder of the structure analysis, since this was compatible with data reported previously for the $A_3BC_{10}O_{20}$ -type structures (2–4). The structure was solved using direct methods and refined by the full-matrix least-squares on F^2 technique for all of the data. Three refinement trials were completed, involving different treatments of disordering at the $Ba(2)$ and/or $Ga(1)$ sites. The refinement parameters in each case included occupancy factors, anisotropic thermal parameters, and correction for secondary extinction. The space group and structure determination as well as the refinement calculations and all structure plots which appear in this paper were performed using Siemens' SHELXTL 5.05 package for DOS on a Gateway 2000 PC-90XL computer. Crystal data and refinement results are summarized in Table 1 for each of the three trials.

RESULTS AND DISCUSSION

Refinement

From the initial structure solution obtained via the direct methods calculation, the $Ba(1)$ position and all four Ga

TABLE 1
Summary of Crystal Data and Refinement Results

Structural formula	Ba ₂ BiGa ₁₁ O ₂₀
Formula weight	1570.58
Color and habit	Yellowish-brown, irregular polygonal platelet
Crystal size (mm ³)	0.33 × 0.26 × 0.03
Space group	<i>I</i> 2/ <i>m</i> (No. 12)
<i>a</i> (Å)	14.9283(14)
<i>b</i> (Å)	11.7046(8)
<i>c</i> (Å)	5.1170(5)
β (deg)	91.137(7)
<i>V</i> (Å ³)	893.92(14)
<i>Z</i>	2
ρ_{calc} (g/cm ³)	5.835
$\lambda(\text{MoK}\alpha)$ (Å)	0.71073
μ (mm ⁻¹)	30.506
θ range for data collection (deg)	2.21–29.99
Limiting indices	–21 ≤ <i>h</i> ≤ 21, –16 ≤ <i>k</i> ≤ 16, –7 ≤ <i>l</i> ≤ 7
Reflections collected	2794
Independent reflections	1361 (<i>R</i> _{int} = 0.0245)
Parameters (Trial 1/Trial 2/Trial 3)	106/102/104
Trial 1 Refinement Results	
Final <i>R</i> indices [<i>I</i> > 2σ(<i>I</i>)]	<i>R</i> ₁ (<i>F</i>) ^{<i>a</i>} = 0.0687, <i>wR</i> ₂ (<i>F</i> ²) ^{<i>b</i>} = 0.1856
Final <i>R</i> indices (all data)	<i>R</i> ₁ (<i>F</i>) ^{<i>a</i>} = 0.0701 <i>wR</i> ₂ (<i>F</i> ²) ^{<i>b</i>} = 0.1865
Goodness-of-fit on <i>F</i> ²	1.274
Extinction coefficient	0.0025(4)
Largest diffraction peak and hole	2.731 and –3.698 e Å ⁻³
Trial 2 Refinement Results	
Final <i>R</i> indices [<i>I</i> > 2σ(<i>I</i>)]	<i>R</i> ₁ (<i>F</i>) ^{<i>a</i>} = 0.0696, <i>wR</i> ₂ (<i>F</i> ²) ^{<i>b</i>} = 0.1847
Final <i>R</i> indices (all data)	<i>R</i> ₁ (<i>F</i>) ^{<i>a</i>} = 0.0709, <i>wR</i> ₂ (<i>F</i> ²) ^{<i>b</i>} = 0.1856
Goodness-of-fit on <i>F</i> ²	1.216
Extinction coefficient	0.0023(4)
Largest diffraction peak and hole	3.150 and –3.880 e Å ⁻³
Trial 3 Refinement Results	
Final <i>R</i> indices [<i>I</i> > 2σ(<i>I</i>)]	<i>R</i> ₁ (<i>F</i>) ^{<i>a</i>} = 0.0676, <i>wR</i> ₂ (<i>F</i> ²) ^{<i>b</i>} = 0.1793
Final <i>R</i> indices (all data)	<i>R</i> ₁ (<i>F</i>) ^{<i>a</i>} = 0.0689, <i>wR</i> ₂ (<i>F</i> ²) ^{<i>b</i>} = 0.1802
Goodness-of-fit on <i>F</i> ²	1.099
Extinction coefficient	0.0023(4)
Largest diffraction peak and hole	2.503 and –3.814 e Å ⁻³

^{*a*}*R*₁(*F*) = $\sum ||F_o| - |F_c|| / \sum |F_o|$ with *F*_o > 4.0σ(*F*).
^{*b*}*wR*₂(*F*²) = $[\sum [w(F_o^2 - F_c^2)^2] / \sum [w(F_o^2)^2]]^{1/2}$ with *F*_o > 4.0σ(*F*) and *w*⁻¹ = σ²(*F*_o)² + (*WP*)² + *TP*, where *P* = (max(*F*_o², 0) + 2*F*_o²)/3, *W* = 0.0924, 0.0944, and 0.0977, and *T* = 71.76, 85.02, and 112.53 for Trials 1, 2, and 3, respectively.

positions expected by analogy to the *A*₃*BC*₁₀O₂₀-type structures were assigned. Another position close to that expected for Ba(2) was found to give slightly better *R* values if refined as a Bi site. This site will subsequently be referred

to as the Bi(1) site. Refinement of these six metal atom positions gave *R*₁ = 0.2604 and *wR*₂ = 0.6512.² Following refinement of the oxygen positions expected from the model compound, a strong residual Fourier peak near the Bi(1) position (at a distance of 0.504 Å) was assigned as Ba(2). The occupancies of the Bi(1) and Ba(2) sites were each reduced by a factor of two, thereby assuming a site occupancy of one-half for each of these two atoms. This resulted in a significant drop in the *R*₁ and *wR*₂ values to 0.1011 and 0.3215, respectively, indicating that Ba(2) does indeed share a site with at least one displaced Bi atom. The refined Ba(2) position was at the site expected from the model compound, with Bi(1) displaced 0.493 Å roughly toward the positive *c* direction.

Following refinement of the displaced bismuth position and all the positions expected from the model compound, two residual peaks remained with sufficient electron density (viz., 6.82 and 4.05 e Å⁻³) to warrant further investigation. Three different refinement trials were completed from this point, each involving a different treatment of the two relatively strong residual peaks: Trial 1 involved refinement of both peaks; Trial 2 involved refinement of only the stronger of the two peaks; and neither of the peaks was refined for Trial 3. The following summarizes the results of each of these refinement scenarios.

Trial 1. One of the peaks was 1.028 Å from the Ba(2) position (and 0.556 Å from Bi(1)) and was assigned as Bi(2). Refinement of this position yielded only a slight drop in *R*₁ and *wR*₂ values. The Bi(1) and Bi(2) positions were each on 4*i* sites, with three nearest-neighbor oxygen atoms and presumably the 6*s*² lone pair as a fourth ligand. The second peak was displaced 0.474 Å away from Ga(1) and was also refined as a Bi site (i.e., Bi(3)) with a low occupancy of 0.1 atom per unit cell. This site had six nearest oxygen neighbors, with three of them at a distance of less than 2 Å, so they are not likely to be Bi–O bonds. Thus, the presence of Bi at the site would require that these three closest oxygen positions be partially vacant. In addition, several instabilities were encountered during refinement. First, the occupancies of the Bi(2) and Bi(3) sites could not be refined simultaneously with Ga(1) or Ba(2) occupancies without causing the refinement to blow up. Second, it was necessary to restrain the temperature factors of the three different Bi atoms to be equal to maintain stability of the refinement. Finally, Ba(2) could not be refined anisotropically without yielding a nonpositive definite solution, and so was refined isotropically. The final refinement data for this trial are given in Table 1.

Trial 2. During the course of refinement for Trial 1, it was observed at one point that the Bi(1) and Bi(2) positions

²Unless otherwise stated, these and all subsequent *R*₁ and *wR*₂ values reported herein are based on all data.

approached to nearly 0.2 Å apart, indicating they might refine as one position. Thus the Bi(2) position was not refined in this trial. Also, since there was no evidence of the oxygen vacancies required to accommodate Bi(3) in Trial 1, the residual peak near the Ga(1) site was refined as a partially shifted gallium position (labeled Ga(1A)) instead. For this refinement, neither the Ga(1) nor Ga(1A) position could be refined anisotropically without resulting in a nonpositive definite solution, so these two positions were refined isotropically. Also the displacement parameters for Ga(1) and Ga(1A) were restrained to be equal; otherwise the displacement parameter for Ga(1A) dropped to zero. The final refinement data are given in Table 1.

Trial 3. Since there were instabilities in the Trial 1 and 2 refinements, a third trial was completed in which neither of the residual peaks just described was refined. Thus, the only bismuth site refined for this trial was again Bi(1), and the result was a more stable refinement with slightly lower *R* values, as indicated in Table 1. All occupancies in this case could be successfully refined simultaneously until the last stage of the calculations. Then, prior to refining Ba(2) anisotropically, it was necessary to fix the Ba(2) and Bi(1) occupancies to prevent the occurrence of a nonpositive definite solution, probably due to the disordered nature of the Ba(2) site. Following refinement of anisotropic displacement parameters for all atoms, as well as secondary extinction, the refinement converged at $R_1 = 0.0689$ and $wR_2 = 0.1802$ for all data.

Since the Trial 3 refinement was more stable, gave *R* values similar to those of the other trials, and offered the simplest model, it was chosen as the best one for describing

the structure of the compound studied in this paper. It should be emphasized, however, that this choice does not necessarily suggest that other Bi sites (at lower occupancies) are not present, just that refinement of such sites offers no advantages in overall refinement outcomes based on the available data. Indeed, following convergence for this refinement, four of the five largest residual peaks (ranging from 2.50 to 1.93 e Å⁻³) were closest to the Ba(2) site, suggesting possibly that the bismuth atoms near this site are disordered. Note, however, that no superlattice reflections were observed in precession photographs or electron diffraction patterns, so that any disorder present is randomized.

Atomic coordinates, occupation factors, and anisotropic and equivalent isotropic displacement parameters from the Trial 3 refinement are listed in Table 2. From the table, it is seen that the refined occupation factors for Trial 3 yield an average composition of Ba_{2.04}Bi_{0.93}Ga_{11.11}O_{20.31}, which agrees with the ideal composition of Ba₂BiGa₁₁O₂₀, taking into account the errors given for the occupation factors. The fact that Ga(1) and Ga(2) have slightly higher than expected occupancies suggests that these sites may be partially occupied by bismuth atoms. Note that in Ba₃TiAl₁₀O₂₀, for example, it is the Al(1) and Al(2) sites which are partially occupied by titanium atoms. Since practically all of the bismuth atoms expected from the ideal composition of the structure appear to be positioned near the Ba(2) site, however, any occupancy of bismuth at the Ga(1) and Ga(2) sites would be small, and so bismuth was not refined at these positions.

The displacement parameters listed in Table 2 reflect the relative magnitudes expected by comparison to the isotropic displacement parameters for Ba₃TiAl₁₀O₂₀, given by Cadée

TABLE 2
Positional, Occupation,^a and Anisotropic^b and Equivalent Isotropic^c Displacement Parameters (Å² × 10⁴) from Trial 3 Refinement

Atom	Site	No. per unit cell	<i>x</i>	<i>y</i>	<i>z</i>	<i>U</i> ₁₁	<i>U</i> ₂₂	<i>U</i> ₃₃	<i>U</i> ₁₂	<i>U</i> ₁₃	<i>U</i> ₂₃	<i>U</i> (eq)
Ba(1)	2 <i>a</i>	2.009(23)	0	0	0	8(1)	20(1)	18(1)	0	5(1)	0	16(1)
Ba(2)	4 <i>i</i>	2.069(141)	0.2825(2)	0	0.0344(6)	5(1)	14(1)	11(1)	0	7(1)	0	10(1)
Bi(1)	4 <i>i</i>	1.853(121)	0.2885(2)	0	0.9395(5)	9(1)	8(1)	22(1)	0	6(1)	0	13(1)
Ga(1)	2 <i>b</i>	2.143(36)	0	½	0	8(1)	5(1)	10(1)	0	7(1)	0	8(1)
Ga(2)	4 <i>h</i>	4.079(52)	0	0.6355(1)	½	5(1)	7(1)	7(1)	0	1(1)	0	6(1)
Ga(3)	8 <i>j</i>	8.000(82)	0.3536(1)	0.3623(1)	0.0100(2)	7(1)	6(1)	7(1)	0(1)	1(1)	0(1)	7(1)
Ga(4)	8 <i>j</i>	7.989(80)	0.1357(1)	0.2876(1)	0.9779(2)	7(1)	7(1)	5(1)	0(1)	1(1)	0(1)	6(1)
O(1)	4 <i>i</i>	4.315(284)	0.4329(10)	0	0.8325(30)	30(8)	9(6)	30(8)	0	8(6)	0	23(4)
O(2)	4 <i>i</i>	4.306(262)	0.9003(9)	0	0.4194(28)	17(7)	8(6)	28(7)	0	6(5)	0	18(4)
O(3)	8 <i>j</i>	8.000(388)	0.2374(7)	0.3670(9)	0.8893(24)	13(5)	17(5)	42(7)	3(4)	-6(4)	-4(4)	24(3)
O(4)	8 <i>j</i>	8.000(347)	0.4183(6)	0.2487(8)	0.8433(17)	7(4)	14(5)	15(4)	-1(3)	2(3)	8(3)	12(3)
O(5)	8 <i>j</i>	8.000(347)	0.8533(8)	0.1476(8)	0.8705(17)	38(6)	7(4)	6(4)	4(4)	5(4)	4(3)	17(3)
O(6)	8 <i>j</i>	8.000(388)	0.9279(7)	0.3817(9)	0.8130(21)	24(6)	11(5)	26(6)	4(4)	15(4)	4(4)	20(3)

^a The occupancy factors for Ba(2) and Bi(1) were fixed toward the end of the refinement (see text). The deviations given for occupancies of these two sites are therefore from earlier in the refinement.

^b The anisotropic thermal parameter is expressed as $\exp[-2\pi^2(h^2a^{*2}U_{11} + k^2b^{*2}U_{22} + l^2c^{*2}U_{33} + 2hka^*b^*U_{12} + 2hla^*c^*U_{13} + 2klb^*c^*U_{23})]$.

^c *U*(eq) is defined as one-third of the trace of the *U*_{*ij*} orthogonalized tensor.

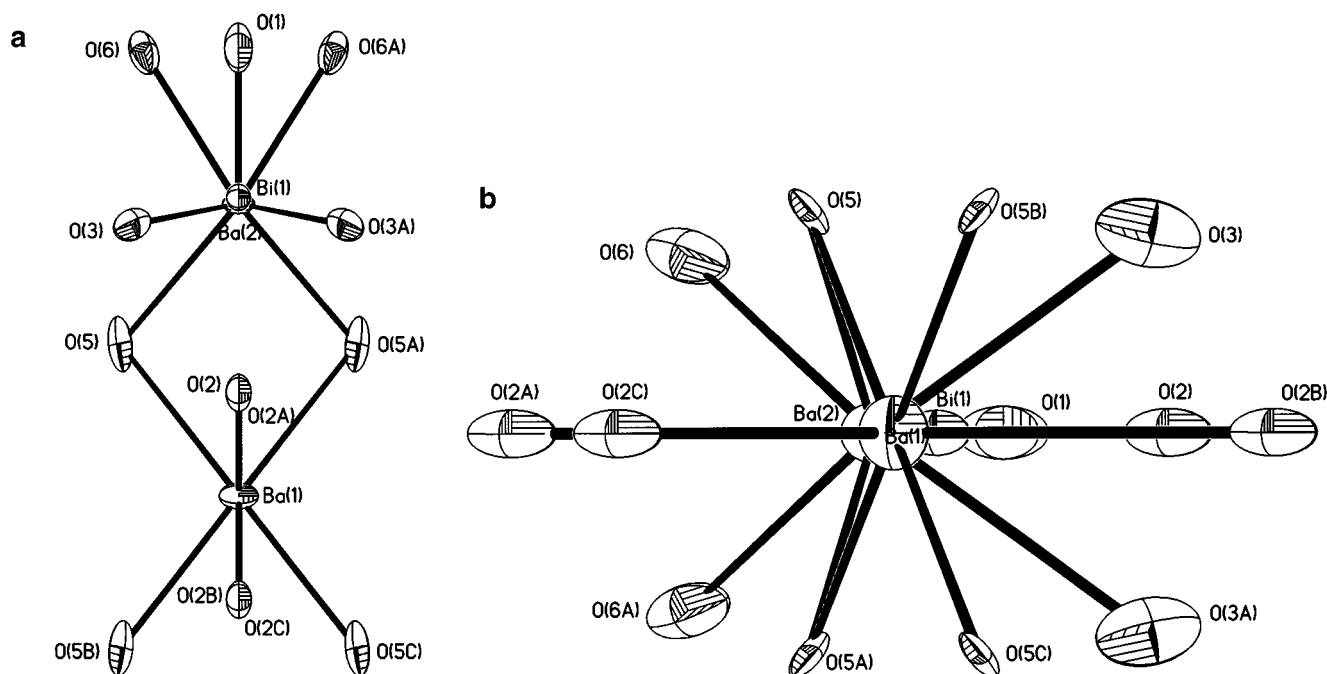


FIG. 3. Localized ORTEP-type plots for the Ba(2) and Ba(1) sites (75% ellipsoids): (a) [001] projection; (b) [100] projection.

et al. (3). Further examination of the data reveals relatively large anisotropic displacement parameters for Bi(1) and most of the oxygen atoms, as shown in Fig. 3. The figure shows that the displacement of oxygen atoms tends to be largest toward the Ba(2)/Bi(1) site. This is expected since the average oxygen positions revealed by the X-ray data should change slightly, depending upon whether Ba(2) or Bi(1) is present at a particular site. Note that O(5) is the only type of oxygen atom bonded to both Ba(1) and Ba(2), and its displacement is intermediate between these two sites. Regarding the Bi(1) displacement, this is largely parallel to the direction of Ba(2) and could reflect some disorder around the Bi(1) site as suggested by the close proximity of the peak refined as Bi(2) in the Trial 1 refinement.

Structure Description and Analysis

The structure resulting from the Trial 3 refinement is shown in Fig. 4a, projected along [001]. Figure 4b is in the same projection as Fig. 4a and shows the position of Bi(1) relative to Ba(2). Figure 4c then shows the relative Ba(2) and Bi(1) positions in the [100] projection. It is seen from the figures that Bi(1) is displaced such that the $6s^2$ lone pair is directed toward the Ba(2) site, with the three nearest oxygen atoms all located on the opposite side of Bi(1). This one-sided coordination is typical for trivalent bismuth atoms displaying steric effects of the $6s^2$ lone pair (5).

Distances and bond angles for both the Bi(1) and Ba(2) positions are given in Table 3. Examination first of the data

for Bi(1) indicates that the Bi–O bonded distances are reasonable in magnitude, given that 2.2 Å can be taken as the ideal average bond length for trivalent bismuth bound to four oxygens.³ Some elongation of Bi–O bond lengths relative to this ideal value would be expected for this case, in which one of the four “ligands” is the stereochemically active lone pair. The Bi(1)–O bond angles seen in Table 3 are compatible with the well-known Gillespie and Nyholm (6) model, predicting that lone pair–bonding pair interactions are stronger than bonding pair–bonding pair interactions. The large range of the angles (as well as distances), however, indicates that the coordination environment of Bi(1) is distorted. This observation is perhaps best accounted for using an alternative approach to the Gillespie–Nyholm model proposed by Hyde and Andersson (7). They found that a stereochemically active lone pair is roughly of the same size as the anion and is positioned at the corner of the regular polyhedron (e.g., a tetrahedron). Since the lone pair–nucleus attraction is stronger than the bonding pair–nucleus attraction, they concluded that the cation must be off center in the polyhedron. As a result, the coordination polyhedra of cations with stereochemically lone pairs are generally distorted. Thus, based on the foregoing discussion, it appears that Bi(2) has shifted from the Ba(2) site to

³ This value was determined by assuming a bond strength of 3/4 for each of four Bi³⁺–O bonds in an ideal coordination environment and then calculating the corresponding bond length using the empirical parameters and equation proposed by Brown and Altermatt (8).

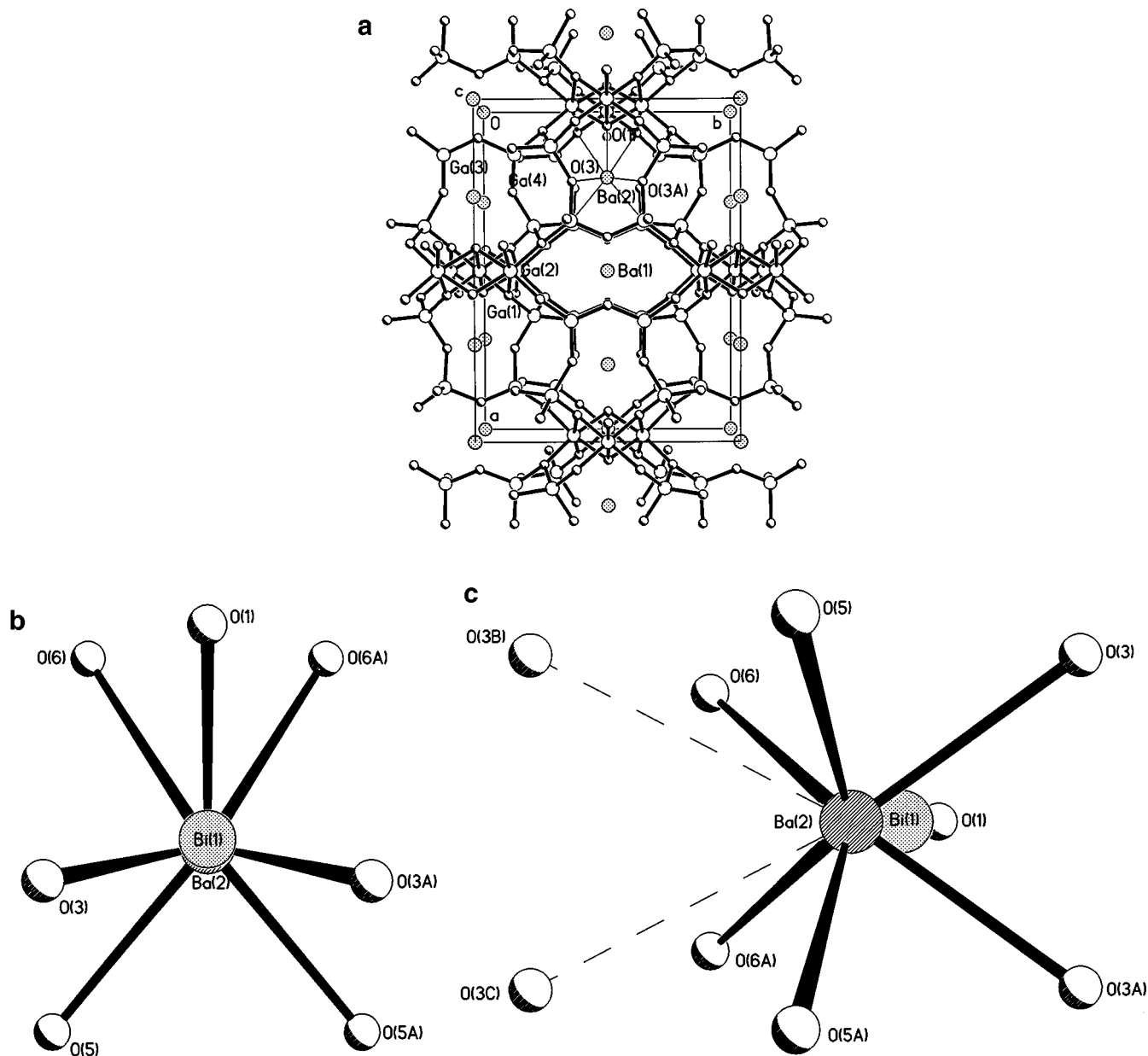


FIG. 4. Structure plots for the final (Trial 3) structure: (a) full plot in the [001] projection (Bi atoms not shown; Ba–O bonds are drawn at one of the Ba(2) sites); (b) localized plot in identical orientation to (a) showing the relative positions of the Ba(2) and Bi(1) atoms; (c) localized plot showing relative positions of the Ba(2) and Bi(1) atoms in the [100] projection. Dashed lines indicate weak, nonbonded interactions.

a suitable coordination environment which preserves site symmetry and satisfies the crystal chemical requirements of bond distances and angles imposed by its stereochemically active lone pair.

The impact that the presence of bismuth has on the local structure can be seen by comparing the distances and angles at the Ba(2) site in the present compound to that in $\text{Ba}_3\text{TiAl}_{10}\text{O}_{20}$, in which the Ba(2) is solely occupied by barium. The relevant data are given in Table 3. Here, the distances for $\text{Ba}_3\text{TiAl}_{10}\text{O}_{20}$ were taken from the data of

Cadée *et al.* (3), and the angles were calculated from their reported positions. It is first of all seen that the Ba(2)–O bond distances in $\text{Ba}_2\text{BiGa}_{11}\text{O}_{20}$ are shorter than in $\text{Ba}_3\text{TiAl}_{10}\text{O}_{20}$, despite the larger cell parameters of the former compound compared to the latter compound (with $a = 14.888 \text{ \AA}$, $b = 11.363 \text{ \AA}$, $c = 4.978 \text{ \AA}$, and $\beta = 90.82^\circ$). This effect is more pronounced for the Ba(2)–O bonds with oxygens common to bismuth. The O–Ba–O angles of the two compounds are very similar and indicate a slight shift in the Ba(2) position toward Bi(1), because the bond angles are

TABLE 3
Distances and Angles for the Ba(2)/Bi(1) Site in Ba₂BiGa₁₁O₂₀
and Ba₃TiAl₁₀O₂₀

Bond or angle	Ba ₂ BiGa ₁₁ O ₂₀	Ba ₃ TiAl ₁₀ O ₂₀ ^a
	Distances (Å)	
Bi(1)–O(1)	2.235(15)	
–O(3), O(3A)	2.319(11)	
–O(5), O(5A)	2.913 (nonbonded)	
–O(6), O(6A)	3.122 (nonbonded)	
Ba(2)–O(1)	2.490(15)	2.611(9)
–O(3), O(3A)	2.681(12)	2.852(6)
–O(5), O(5A)	2.715(10)	2.736(7)
–O(6), O(6A)	2.922(12)	3.012(8)
–O(3B), O(3C)	3.382 (nonbonded)	3.124(7)
	Angles (deg)	
O(1)–Bi(1)–O(3)	88.29(41)	
O(3)–Bi(1)–O(3A)	84.32(58)	
O(1)–Ba(2)–O(3)	75.59(38)	74.09
O(3)–Ba(2)–O(3A)	70.98(50)	70.11
O(5)–Ba(2)–O(5A)	79.01(44)	79.45
O(5)–Ba(2)–O(6)	99.29(30)	99.68
O(5)–Ba(2)–O(6A)	139.84(30)	139.17
O(1)–Ba(2)–O(6)	62.30(36)	61.20
O(3)–Ba(2)–O(5)	72.80(31)	74.94

^aDistances taken from ref 3; angles calculated from positions given in ref 3.

larger on the bismuth side and smaller on the non-bismuth side relative to the same angles in Ba₃TiAl₁₀O₂₀. The Ba(2) coordination environment of Ba₃TiAl₁₀O₂₀ is exactly as shown in Fig. 4c for Ba₂BiGa₁₁O₂₀, except the dashed lines to two of the O(3) atoms are now reported as actual bonds. Note that the O(3B) and O(3C) atoms in the present structure are partially bound to Bi in the adjacent unit cell, so they appear to have shifted away from Ba(2). Thus the principal effect resulting from the presence of bismuth appears to be a reduction of coordination of Ba(2) from 9 to 7. Of course, it is difficult to say exactly where to stop regarding an O atom as coordinating to Ba(2). Certainly the interactions between Ba(2) and the O(3B) and O(3C) atoms are real, although relatively weak.

The Ba(1)–O and Ga–O bond distances in Ba₂BiGa₁₁O₂₀ are listed in Table 4 and are seen to be within typical ranges based on values observed in similar structures (3, 4). A good check of the overall structure is given by computing bond valence sums for all atoms using the distances listed in Tables 3 and 4. Individual bond valences are obtained using the expression proposed by Brown and Altermatt (8):

$$v_{ij} = \exp[(r_0 - r_{ij})/0.37],$$

where r_0 is an empirical parameter characteristic of the atom pair forming the bond and r_{ij} is the experimental bond distance. For Bi–O, Ba–O, and Ga–O bonds, Brown and Altermatt (8) give r_0 values of 2.094, 2.285, and 1.730 Å,

TABLE 4
Interatomic Distances (Å) in Ba₂BiGa₁₁O₂₀

Ba(1)–O(2)	2.636(14)	2 ×
–O(5)	2.857(11)	4 ×
Ga(1)–O(1)	1.991(15)	2 ×
–O(6)	1.987(10)	4 ×
Ga(2)–O(1)	2.053(10)	2 ×
–O(4)	1.961(9)	2 ×
–O(6)	1.957(10)	2 ×
Ga(3)–O(2)	1.820(6)	1 ×
–O(3)	1.830(10)	1 ×
–O(4)	1.861(9)	1 ×
–O(5)	1.848(9)	1 ×
Ga(4)–O(3)	1.845(11)	1 ×
–O(4)	1.865(9)	1 ×
–O(5)	1.819(9)	1 ×
–O(6)	1.817(10)	1 ×

respectively. The total bond valence for each atom is then given by simply summing the individual bond valences around it. The results for Ba₂BiGa₁₁O₂₀ are given in Table 5. For each of the four gallium positions and most of the oxygen sites, the bond valence sums are very close to the expected ideal values (i.e., the respective oxidation numbers). The largest deviations observed are for the bismuth and both barium positions. The Bi(1) sum of 1.771 is far lower than the expected value of 3.0; however, these calculations do not take into account that the stereochemically active 6s² lone pair acts effectively as a ligand in this case. That the Bi–O bond lengths are reasonable is indicated by the fact that the O(1) and O(3) sites have nearly ideal valence sums when bound to Bi(1). The Ba(2) site is overbonded, as expected from the earlier discussion of the decreased average Ba(2)–O bond lengths due to the presence of Bi. Finally, the Ba(1) site is somewhat underbonded, also due to the presence of bismuth. The four O(5) atoms which are part of the Ba(1) coordination sphere are shared with adjacent Ba(2) sites, with two O(5) atoms bonded to the Ba(2) atoms above and two bonded to the Ba(2) atoms below the Ba(1) site. Since the Ba(2)–O(5) bonds have on average decreased, the Ba(1)–O(5) bonds appear relatively elongated. This in turn yields the observed less-than-ideal valence sum for Ba(1).

SUMMARY

The structure of Ba₂BiGa₁₁O₂₀ described in this paper is very similar to that of A₃BC₁₀O₂₀-type compounds, based on earlier structure refinements for compositions A = Pb and Ba, B = Ge, Sn, and Ti, and C = Al, Ga, and Fe as well as several other related compositions by analogy (2–4). The major difference is that the Bi atom is located near the Ba(2) site, whereas the B-type (i.e., tetravalent) atoms share sites with C(1)- and C(2)-type atoms. The displacement of the Bi

TABLE 5
Valence Bond Sums (V_{ij}) For $Ba_2BiGa_{11}O_{20}$

Cations	$v_{ij} = v_{ji}$ Anions						$V_{ij} = \sum v_{ij}$, for Cations (\rightarrow)
	O(1) ^a	O(2)	O(3) ^a	O(4)	O(5)	O(6)	
Ba(1)		0.387 ($\times 2$) \rightarrow ($\times 1$) \downarrow			0.213 ($\times 4$) \rightarrow ($\times 1$) \downarrow		1.626
Ba(2)	0.575 ($\times 1$) \rightarrow ($\times 1$) \downarrow		0.343 ($\times 2$) \rightarrow ($\times 1$) \downarrow		0.313 ($\times 2$) \rightarrow ($\times 1$) \downarrow	0.179 ($\times 2$) \rightarrow ($\times 1$) \downarrow	2.245
Bi(1)	0.683 ($\times 1$) \rightarrow ($\times 1$) \downarrow		0.544 ($\times 2$) \rightarrow ($\times 1$) \downarrow				1.771
Ga(1)	0.494 ($\times 2$) \rightarrow ($\times 1$) \downarrow					0.499 ($\times 4$) \rightarrow ($\times 1$) \downarrow	2.984
Ga(2)	0.418 ($\times 2$) \rightarrow ($\times 2$) \downarrow			0.536 ($\times 2$) \rightarrow ($\times 1$) \downarrow		0.541 ($\times 2$) \rightarrow ($\times 1$) \downarrow	2.990
Ga(3)		0.784 ($\times 1$) \rightarrow ($\times 2$) \downarrow	0.763 ($\times 1$) \rightarrow ($\times 1$) \downarrow	0.702 ($\times 1$) \rightarrow ($\times 1$) \downarrow	0.727 ($\times 1$) \rightarrow ($\times 1$) \downarrow		2.976
Ga(4)			0.733 ($\times 1$) \rightarrow ($\times 1$) \downarrow	0.694 ($\times 1$) \rightarrow ($\times 1$) \downarrow	0.786 ($\times 1$) \rightarrow ($\times 1$) \downarrow	0.790 ($\times 1$) \rightarrow ($\times 1$) \downarrow	3.003
$V_{ij} = \sum v_{ij}$, for Anions (\downarrow)	with Ba(2) 1.905 with Bi(1) 2.013	1.955	with Ba(2) 1.839 with Bi(1) 2.040	1.932	2.039	2.010	

^a Anion sums are given for both cases of O(1) and O(3) bound to either Ba(2) or Bi(1).

atoms relative to the Ba(2) site is due to the presence of the stereochemically active $6s^2$ lone pair, as indicated by crystal chemical analysis of the Ba(2)/Bi(1) site. The model is supported by a bond valence sum analysis of the overall structure. This is apparently the first structure report of an $A_2BC_{11}O_{20}$ -type composition.

ACKNOWLEDGMENTS

The authors are grateful to Dr. John Hughes for helpful discussions and for obtaining precession data and to Dr. Allen Hunter for reviewing the manuscript. This work was partially supported by Youngstown State University Research Grant No. 887 and made use of the X-ray facility established at Youngstown State University in part by Grant DMR-9403889 from the National Science Foundation and by Grant CAP-098 from the Ohio Board of Regents Action Fund.

REFERENCES

1. F. Haberey, R. Leckebusch, M. Rosenberg, and K. Sahl, *J. Cryst. Growth* **61**, 284 (1983).
2. H. Vinek, H. Völlenkne, and H. Nowotny, *Monatsh. Chem.* **101**, 275 (1970).
3. M. C. Cadée, D. J. W. IJdo, and G. Blasse, *J. Solid State Chem.* **41**, 39 (1982).
4. M. C. Cadée, G. C. Verschoor, and D. J. W. IJdo, *Acta Crystallogr., Sect. C* **39**, 921 (1983).
5. R. Enjalbert, G. Hasselmann, and J. Galy, *J. Solid State Chem.* **131**, 236 (1997).
6. R. J. Gillespie and R. S. Nyholm, *Q. Rev. Chem. Soc.* **11**, 339 (1957).
7. B. G. Hyde and S. Andersson, in "Inorganic Crystal Structures," pp. 257-260. Wiley, New York, 1989.
8. I. D. Brown and D. Altermatt, *Acta Crystallogr., Sect. B* **41**, 244 (1985).